Inorg. Chem. **2003**, *42*, 6673–6681

Nine Hexagonal Ca_5Pb_3Z Phases in Stuffed Mn_5Si_3-Type Structures with Transition Metal Interstitial Atoms *Z*. Problems with Classical Valence States in Possible Zintl Phases

Arnold M. Guloy,[†] Anja-Verena Mudring,[‡] and John D. Corbett*[,‡]

Department of Chemistry and Ames Laboratory—DOE,[1] Iowa State University, Ames, Iowa 50011, and Department of Chemistry, University of Houston, Houston, Texas 77024-5641

Received May 27, 2003

Ternary hexagonal Ae_5Tt_3Z phases have been obtained from high-temperature reactions (1000–1300 °C in Ta) only for Ae (alkaline-earth metal) = Ca, Tt (tetrel) = Pb, and Z = V, Cr, Mn, Fe, Co, Ni, Zn, Ru, or Cd. The hexagonal crystal structures (stuffed Mn_5Si_3-type, $P6_3/mcm$, Z = 2) were refined for Z = Mn and Fe (a = 9.3580(3), 9.3554(5) Å, c = 7.009(1), 7.009(1) Å, respectively). In contrast, Ca_5Pb_3Z for Z = Cu or Ag form only with a trigonal structure ($P\bar{3}c1$, Z = 2, a = 9.4130(3) Å, c = 7.052(1) Å for Cu) in which regular displacements of only the linear strings of Ca1 atoms occur. The existence of these compounds stands in contrast to the nonexistence of all binary Ae_5Tt_3 products from Ca to Ba (Ae) and Si to Pb (Tt) with a Mn_5Si_3-type structure. Therefore, it once seemed attractive to consider the Z elements in these Ca_5Pb_3Z compounds as reducing agents (electron donors). The Mn and Fe structures appropriately exhibit greatly enlarged antiprismatic calcium cavities about Z. Other indications of relatively electron-poor environments around Fe are found in its properties, which include soft ferromagnetism with an elevated magnetic moment (6.3 μ_B) and a large Fe $3p_{3/2}$ binding energy relative to that in La_5Ge_3Fe, $La_{15}Ge_9Fe$, etc. The Ca_5Pb_3Mn phase exhibits metallic behavior (ρ_{295} = 135 $\mu\Omega$ cm) and temperature-independent Pauli paramagnetism. These properties are supported by ab initio band structure calculations for Ca_5Pb_3Mn, which show strong Ca–Pb bonding and a broad Pb-based band, with appreciable Ca–Mn and Ca–Pb bonding states at and above E_F. Distortion of the Cu analogue gives strengthened Ca–Pb bonding and reduced Cu–Ca1 repulsions. A Zintl phase description of these compounds and some releated compounds in terms of closed Pb bands is not appropriate.

Introduction

As recently reviewed,[2] a great deal of experience has been accumulated concerning the interstitial chemistry of T_5M_3 host compounds with the hexagonal Mn_5Si_3-type structure.[3–9] The essential feature of this structure is the presence of infinite $T_{6/2}M_3$ chains of confacial antiprisms of the more electropositive (transition or alkaline-earth) metal T on which the shared edges are bridged by isolated p-element atoms (anions) M, Figure 1. A great many interstitial T_5M_3Z derivatives with a stuffed Mn_5Si_3 structure may be synthesized in which a variety of Z atoms center all antiprisms. The binary hosts are evidently all electron rich when oxidation states are assigned in a conventional manner, and all that have been tested are appropriately metallic. The number of surplus electrons relative to simple octet requirements for the isolated main-group atom components naturally diminish for either electron-poorer M or T.

The interstitial chemistry that is most relevant to the present research has been most thoroughly investigated for La_5Tt_3 hosts, Tt (tetrel) = Ge or Pb,[8,9] as well as for Ae_5-

* Author to whom correspondence should be addressed. E-mail: jdc@ameslab.gov.
† University of Houston.
‡ Iowa State University.

(1) This research was supported by the Office of the Basic Energy Sciences, Materials Sciences Division, U. S. Department of Energy. The Ames Laboratory is operated for DOE by Iowa State University under Contract WB7405-Eng-82.

(2) Corbett, J. D.; Garcia, E.; Guloy, A. M.; Hurng, W.-M.; Kwon, Y.-U.; Leon-Escamilla, A. E. *Chem. Mater.* **1998**, *10*, 2824.
(3) Hurng, W.-M.; Corbett, J, D. *Chem. Mater.* **1989**, *1*, 1.
(4) Garcia, E.; Corbett, J. D. *Inorg. Chem.* **1990**, *29*, 3274.
(5) Kwon, Y.-U.; Rzeznik, M. A.; Guloy, A.; Corbett, J. D. *Chem. Mater.* **1990**, *2*, 546.
(6) Kwon, Y.-U.; Corbett, J. D. *Chem. Mater.* **1992**, *4*, 1349.
(7) Kwon, Y.-U.; Corbett, J. D. *J. Alloys Compd.* **1993**, *190*, 219.
(8) Guloy, A. M.; Corbett, J. D. *Inorg. Chem.* **1993**, *32*, 3532.
(9) Guloy, A. M.; Corbett, J. D. *J. Solid State Chem.* **1994**, *109*, 352.

10.1021/ic0301728 CCC: $25.00
Published on Web 09/16/2003

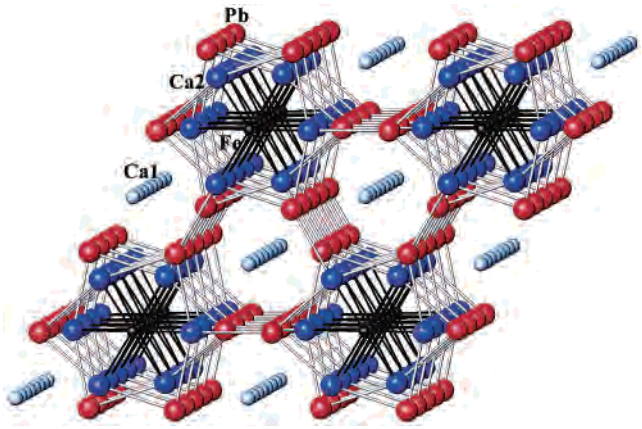

Figure 1. Off-[001] projection of the hexagonal structure of Ca_5Pb_3Fe (isotropic). Chains of confacial $^1_\infty[Ca(2)]_{6/2}$ antiprisms (blue) centered by Fe (black) lie along 0,0,*z*, with all edges of the shared faces bridged by isolated Pb atoms (red). The chains of Ca1 atoms are light blue.

Pn_3Z in which Ae = Ca−Ba, Pn = As−Bi, and Z = Cl, Br, or H.[3,10] A total of 17−19 different interstitial compounds La_5Tt_3Z may be synthesized for each host, generally as stoichiometric phases in which Z may be a pnictogen, chalcogen, halogen, or a late transition metal Mn−Zn. The hosts are generally metallic and many products remain such, although selections of particular nonmetal Z may in special cases also create closed-shell valence compounds (Zintl phases), e.g., for the diamagnetic semiconductors La_5Ge_3P and Ca_5Sb_3Cl but not when Z comes from a metal, i.e., Fe. On the other hand, incorporation of the electron-poorer tetrels Si−Sn as Z in La_5Ge_3 appears to be limited by a simple valence electron count for the host (5·3 − 3·4 = 3), thus allowing only substoichiometric examples such as $La_5Ge_3Si_{0.75}$.[8] Otherwise, fully stoichiometric R_5Tt_4 (or R_5Tt_3Tt') compounds (R = rare-earth element) are always found to occur in other structure types such as Sm_5Ge_4 or Zr_5Si_4. These structures usually feature nominal Tt_2^{-6} dimers, evidently in order to avoid generating holes in the nominal Tt valence band and basically to come closer to Zintl−Klemm concepts.[11] The same concepts apply in principle to a number of Ae_5Tt_3 phases (Ae = alkaline-earth metal) that occur in Cr_5B_3-type structures with equal numbers of monomeric (Tt^{-4}) and dimeric (Tt_2^{-6}) anions and are thus for this charge type nominal Zintl phases with closed shell anions.[12] (The superscripts on these ions of course denote oxidation states, not actual charges.) The list of members includes two phases relevant here, Ba_5Pb_3[13] and Sr_5Pb_3,[14] but both have recently been shown to actually be monohydrides, whereas the simple binaries do not exist with this structure.[15] In other cases, Ca_5Ge_3 for example, the classical Tt_2^{-6} anions have been shown by higher level calculations to be unstable in the cation environment, and so these compounds are metallic and not Zintl in character.[16]

A surprising exception to these observations is the 1963 report of Ca_5Pb_3 in a $\sqrt{3} \times \sqrt{3} \times 1$ superstructure of the Mn_5Si_3 type,[17] which would supposedly leave an incomplete valence shell on Pb (5·2 − 3·4 = −2). However, this structure was established only by X-ray film methods, and the thermal parameters were assigned arbitrarily. A subsequent refinement of the structure of Eu_5As_3 as isostructural with Ca_5Pb_3 had many crystallographic problems as well as unresolved synthetic complications.[18] Our studies of the former compound have revealed that the superstructure has a heavy atom composition nearer $Ca_{5.67}Pb_3$, that is, with self-interstitials $Ca_5Pb_3Ca_{0.67}$ in a distorted Mn_5Si_3-type superstructure in which Pb−Pb bonding appears to complete the electronic conditions for a Zintl phase.[11] However, it was later realized that the $Ca_{5.67}Pb_3$ product may have also contained hydrogen.[15] An earlier assignment of a Mn_5Si_3-type structure to Ca_5Pb_3 according to Debye−Scherrer powder data analysis[19] would not have been able to distinguish the superstructure.

A new postulate, that interstitials with higher-lying electron-donor (valence) states might stabilize an otherwise electron-deficient Mn_5Si_3-type host, was suggested in part by the above $Ca_{5.67}Pb_3$ result, and this encouraged us to explore related ternary Ca−Pb possibilities with better-behaved structures. The present article reports on a series of Ca_5Pb_3Z phases for 3d metal Z that exhibit simple stuffed Mn_5Si_3-type structures. Their existence led us to an early tentative interpretation that the Z atoms were in fact acting as two-electron donors so as to complete the valence electronic requirements of formal Pb^{-4} anions. However, this rather literal interpretation of the bonding in such potential Zintl phases avoids the question as to whether such a closed shell assignment for lead is correct. Higher level calculations regarding this problematic condition are also reported here.

Experimental Section

Materials. All reagents and products were handled and stored in N_2- or He-filled gloveboxes (Dri-Lab, Vacuum Atmospheres) with moisture levels <1 ppm (vol.). Reaction techniques utilizing welded Ta contains together with Guinier powder patterns for both approximate phases analyses and lattice constant refinements (with Si as an internal standard) have been described before.[4,8,10] The calcium metal utilized came from Ames Lab as chunks of triply distilled metal (which should have been relatively free of hydrogen impurities), and this was stored and handled only in a helium-atmosphere glovebox. Lead metal sheet was rolled from electrolytic bar (Ames Lab, 6−9's), and its dark surface was scraped off before use. The potential interstitial elements utilized were high purity reagents with stated metals-basis contents as follows: manganese powder (99.99%), iron chips (99.95%), ruthenium powder (99.999%), nickel sheets (99.99%), copper chips (99.999%), chromium powder (99.99%), vanadium powder (99.999%), magnesium strips (99.999%),

(10) Leon-Escamilla, E. A.; Corbett, J. D. *J. Alloys Compd.* **1998**, *265*, 104.
(11) Guloy, A. M.; Corbett, J. D. Unpublished research.
(12) Schäfer, H. *Annu. Rev. Mater. Sci.* **1985**, *15*, 1.
(13) Sands, D. E.; Wood, D. H.; Ramsey, W. J. *Acta Crystallogr.* **1964**, *17*, 986.
(14) Bruzzone, G.; Franceschi, E.; Merlo, F. *J. Less-Common Met.* **1978**, *60*, 59.
(15) Leon-Escamilla, E. A.; Corbett, J. D. *Inorg. Chem.* **2001**, *40*, 1226.
(16) Mudring, A.-V.; Corbett, J. D. *J. Am. Chem. Soc.* Submitted.
(17) Helleis, O.; Kandler, H.; Leicht, E.; Quiring, W.; Wolfel, E. *Z. Anorg. Allg. Chem.* **1963**, *320*, 86.
(18) Wang, Y.; Calvert, L. D.; Gabe, E. J.; Taylor, J. B. *Acta Crystallogr.* **1978**, *B34*, 2281.
(19) Bruzzone, G.; Merlo, F. *J. Less-Common Met.* **1976**, *48*, 103.

Table 1. Synthesis Conditions, Space Groups, and Lattice Constants for Ca_5Pb_3Z Phases

product[a]	anneal (°C)[b]	space group[c]	*a* (Å)	*c* (Å)	*V* (Å^3)
Ca_5Pb_3V	1300	$P6_3/mcm$	9.3585 (2)	7.011(1)	531.8(1)
Ca_5Pb_3Cr	1300	$P6_3/mcm$	9.3591(2)	7.015(1)	532.1(1)
Ca_5Pb_3Mn	1300	$P6_3/mcm$	9.3580(3)	7.009(1)	531.6(1)
Ca_5Pb_3Fe	1300	$P6_3/mcm$	9.3554(5)	7.009(1)	531.3(1)
Ca_5Pb_3Co	1300	$P6_3/mcm$	9.3547(3)	7.006(1)	530.9(1)
Ca_5Pb_3Ni	1300	$P6_3/mcm$	9.3547(4)	7.0073(7)	531.05(4)
Ca_5Pb_3Cu	850	$P\bar{3}c1$	9.4130(3)	7.052(1)	541.0(3)
Ca_5Pb_3Zn	850	$P6_3/mcm$	9.3626(2)	6.992(1)	530.8(1)
Ca_5Pb_3Ag	850	$P\bar{3}c1$	9.4317(2)	7.055(1)	542.7(1)
Ca_5Pb_3Cd	850	$P6_3/mcm$	9.3705(1)	7.012(1)	533.2(1)
Ca_5Pb_3Ru	1300	$P6_3/mcm$	9.3650(1)	7.028(1)	533.8(1)

[a] Stoichiometric amounts of the elements were loaded except that CaCu, $CaZn_2$, and CaCd were used as reactants where appropriate. [b] Annealed at temperature for 10 days, then slowly cooled in the ranges of 1300−1000 °C or 850−500 °C over 5 days. [c] All products were single phase according to Guinier photographs. Silicon (NIST) was employed as an internal standard for lattice constant refinements; 22 °C, $\lambda = 1.54056$ Å.

cobalt wire (99.99%), silver powder (99.98%), zinc pellets (99.999%), and cadmium strips (99.999%).

Syntheses. All manipulations and weighings were done in a helium-filled glovebox to ensure that the total content of each reaction was known well and that minimum contamination occurred during the handling of the reagents. As is customary, the $^3/_8$-in. o.d. tantalum containers utilized showed no visible attack and retained their ductility through the reactions. Mixtures of the reagents therein on a ~250-mg scale were heated either in a high-temperature vacuum furnace to 1300 °C or in a resistance furnace (inside a sealed silica jacket) to 850 °C, and both were thereafter slowly cooled over 5 days. The former 1300 °C route appeared to be necessary to gain complete reaction between the partially liquid Ca_5Pb_3 composition and the higher melting refractory transition metals V−Ni and Ru, especially when these were not introduced as powders. The temperature regime employed took advantage of the reported phase relationships in the Ca−Pb system,[19] a "Ca_5Pb_3" peritectic at 1127 °C that lies between eutectics at 638 and 750 °C. The use of 1000 °C as a lower limit for cooling avoided the formation of appreciable CaPb at 968 °C. Some Ca_5Pb_3Z (Z = Cu, Zn, Ag, and Cd) compounds could be obtained after slow cooling from 850 °C, although Ca_5Pb_3Ag and Ca_5Pb_3Cu were also produced by the 1300 °C route. All such products were single phase to Guinier (Enraf-Nonius 552) powder diffraction (>~95%) and were markedly less air sensitive than the Ca−Pb binaries. Table 1 lists the reaction temperatures, structure types, and lattice constant information for all of the compounds. As an aside, a surprising structural change was also observed when the synthesis of $Ca_5Pb_3Fe_{0.5}$ was attempted. Both the Guinier patterns and single-crystal precession photographs indicated a doubling of the *c* axis was present, not the $\sqrt{3}$ expansion of *a* and *b* known in another ordered superstructure of such Mn_5Si_3 derivatives ($La_{15}Ge_9Fe$).[20] The new structure has not been studied, but an ordered Fe occupancy and some Pb−Pb bonding therewith may be possible.

Properties. To confirm the stoichiometries, analyses were done for the crystalline Mn, Fe, Co, and Cu congeners with the aid of a JEOL JSM-840 SEM unit equipped with a KEVEX-EDX system, Table 2. Well-faceted crystals were fixed in epoxy, polished with sandpaper and leather, and grounded to the copper holder with silver paint. Samples were examined in the backscattering and topological modes in order to select sites for analysis. The bulk compositions were used for standards whenever possible to avoid matrix errors.

Table 2. SEM Analyses of Some Ca_5Pb_3Z Phases

loaded stoichiometry	atom % Ca	atom % Pb	atom % Z	calcd formula
Ca_5Pb_3Mn	55.2(1)	34.25(5)	10.5(1)	$Ca_5Pb_{3.1}Mn_{0.95}$
Ca_5Pb_3Mn[a]	55.26(4)	33.56(1)	10.73(6)	$Ca_5Pb_{3.04}Mn_{0.97}$
Ca_5Pb_3Fe	56.4(1)	32.73(4)	10.8(1)	$Ca_5Pb_{2.9}Fe_{0.96}$
Ca_5Pb_3Co	55.9(1)	33.56(5)	10.5(1)	$Ca_5Pb_{3.0}Co_{0.93}$
Ca_5Pb_3Cu	55.5(1)	32.22(5)	12.2(1)	$Ca_5Pb_{2.9}Cu_{1.1}$

[a] Sample used for single-crystal refinement (below).

Magnetic susceptibilities were measured between 6 and 300 K on a MPMS SQUID instrument from Quantum Design, usually at 3 T. A container was used in which the sample is held between the flat faces of two 3-mm-diameter SiO_2 rods.[20] Specific electronic resistivities were measured over a 100−300 K range by the "Q" method[21] on sieved (150−250 μm) samples diluted with chromatographic alumina.

X-ray photoelectron spectroscopy (XPS) data for the Fe and Ni phases were secured with the aid of an AEI-200B spectrometer and Al Kα radiation, the binding energies being referenced to adventitious carbon at 285.0 eV. Samples were mounted on indium within an attached glovebox. Argon ion etching was sometimes employed to clean the sample surface. This resulted in larger signals for Z but no significant shift of the core peaks of the constituent atoms.

Computational Details. TB-LMTO-ASA (linear muffin-tin orbital atomic sphere approximation) electronic band structure calculations were carried out for Ca_5Pb_3Mn and Ca_5Pb_3Cu as well as for the hypothetical empty structures using the Stuttgart LMTO47 program.[22] Exchange and correlation effects were treated in a local spin density approximation (LDA).[23] All relativistic effects except spin−orbit coupling were taken into account using a scalar relativistic approximation.[24]

Within the ASA, space is filled with small overlapping Wigner−Seitz (WS) atomic spheres. The symmetry of the potential is considered spherical inside each WS sphere, and a combined correction is used to take into account the overlapping part.[25] The radii of the WS spheres were obtained under the requirement that the overlapping potential is the best achievable approximation to the full potential and were so determined by an automatic procedure described in the last. The maximal overlap should not be too large because the error in the kinetic energy introduced by the combined correction is proportional to the fourth power of the relative sphere overlap. Since the structures under examination are not dense packed, interstitial "empty spheres" (ES) were introduced to achieve space filling with a minimal overlap. The optimal positions and the radii for the empty sphere were determined automatically according to the method described in ref 25.

The basis set of short-ranged atom-centered TB-LMTO's comprised for calcium 4s, 4p, and 3d, for lead 6s, 6p, 6d, and 5f, and for Mn and Cu 4s, 4p, and 3d orbitals. Ca 4p, Pb 6d, and 5f were treated by the Löwdin downfolding technique[22] that allows one to derive few orbital effective Hamiltonians by keeping only the

(20) Guloy, A. M.; Corbett, J. D. *Inorg. Chem.* **1996**, *35*, 4669.
(21) Zhao, J.-T.; Corbett, J. D. *Inorg. Chem.* **1995**, *34*, 378.
(22) (a) Andersen, O. K. *Phys. Rev. B* **1975**, *12*, 3060. (b) Andersen, O. K.; Jepsen, O. *Phys. Rev. Lett.* **1984**, *53*, 2571. (c) Andersen, O. K.; Jepsen, O.; Glötzel, D. In *Highlights of Condensed-Matter Theory*; Bassani, F., Fumi, F., Tosi, M. P., Eds.; Elsevier Science: New York, 1985. (d) Lambrecht, W. R. L.; Andersen, O. K. *Phys. Rev. B* **1985**, *34*, 2439.
(23) von Barth, U.; Hedin, L. *J. Phys. C* **1972**, *5*, 1629.
(24) Koelling, D. D.; Harmon, B. N. *J. Phys. C* **1977**, *10*, 3107.
(25) Jepsen, O.; Andersen, O. K. *Z. Phys. B* **1995**, *97*, 35.

relevant degrees of freedom and integrating out the irrelevant ones. The k-space integrations were performed by the tetrahedron method.[26]

To illustrate the contribution of different atoms to the overall density of states (DOS), energy-resolved and atom-projected densities of states (PDOS) for particular atoms were used. The crystal orbital Hamiltonian population (COHP) method is used for bond analysis.[27] COHP gives the energy contributions for all electronic states for selected bonds by partitioning the band structure energy, hence, the sum of energies of the Kohn−Sham orbitals, in terms of the respective orbital pair contributions. Note that the values are negative for bonding and positive for antibonding interactions, the reverse of the signs used in crystal orbital overlap population (COOP[28]) diagrams in the semiempirical Hückel treatments. This discrepancy emerges from the fact that to obtain the COOP, the DOS gets multiplied by the overlap population whereas for COHP, the weighting the DOS employs the corresponding element of the Hamiltonian. The Fermi level was chosen as an internal reference level in all cases.

Structure Determinations. The hexagonal Mn_5Si_3-type ($P6_3/mcm$) structure type and composition was established by single-crystal means for Ca_5Pb_3Mn and was also confirmed for Ca_5Pb_3Fe. The occurrence of a second small series with a distorted trigonal Mn_5Si_3-related structure ($P\bar{3}c1$) (Table 1) was clarified by a single crystal study of Ca_5Pb_3Cu. All data were collected at room temperature from hexagonal-shaped crystals with the aid of a Rigaku AFC6R diffractometer via $\theta-2\theta$ scans and over four octants to 2θ limits of 70.2, 70.2, and 50°, respectively. Empirical absorption corrections were applied to each data set on the basis of three psi scans. Improved lattice parameters were later calculated for these three by least-squares fittings of Guinier powder data with the aid of lines from the National Institute of Standards and Technology (NIST) standard silicon that was included as an internal standard, and these values were used in all distance calculations. The powder data observed for the remaining analogues of each structure type (Table 1) were carefully compared with powder patterns calculated according to refined structures in order to assign the members to each series. In addition, the absence of any of the known superstructures in 5−3 systems was assured. The samples of Ca_5Pb_3Z for Z = Mn, Fe, and Cu were shiny metallic and brittle crystals, whereas the Ag compound was grayish in color.

Precession photographs of the Ca_5Pb_3Mn crystal established the absence of the $\sqrt{3} \times \sqrt{3}$ expansion found with $La_{15}Ge_9Z$[20] or any other superstructure, and cone and Laue photographs confirmed the presence of the 6-fold axis. Higher level photographs also indicated systematic observation conditions that corresponded to those for space groups $P6_3/mcm$, $P6c2$, and $P6_3/cm$, and this was also confirmed by a careful examination of the single-crystal data. The space group $P6_3/mcm$ and the initial positional parameters from the La_5Ge_3 study[8] were applied on the basis of the many similarities.

Refinement[29] of the Mn data with isotropic thermal parameters resulted in $R = 4.2\%$, $R_w = 5.4\%$. Inclusion of anisotropic parameters led to satisfactory refinement values, $R = 4.0$, $R_w = 4.4\%$, but the ellipsoids for all atoms were elongated along the c axis, the short axis of the crystal ($\mu = 757$ cm^{-1}). Application of DIFABS,[30] starting with the parameters from the isotropic refinement as recommended, produced significant improvements in the thermal parameters and smaller estimated standard deviations. Refinement of variable occupancies for Ca1, Ca2, and Mn, with Pb kept at unity, yielded 0.97(2), 1.00(2), and 0.96(2), respectively, which correspond to $Ca_{4.94(4)}Pb_3Mn_{0.97(3)}$, in excellent agreement with standard electron microscopy (SEM) data (Table 2) and indistinguishable from those for ideal structure. These variables were returned to unity for the final cycles, ($R/R_w = 3.7/3.9\%$), after which a difference Fourier calculation showed the largest residual peak, 2.06 e$^-$/Å^3, lay within 1 Å of Pb. Other structural models that allowed for Ca/Mn or Pb/Mn mixed occupancies and substitutions were evaluated, but their refinements all resulted in significantly higher residuals ($R > 8\%$). The iron compound was found to be very similar in all respects, the final residuals and the largest feature in the difference map being 3.2/3.5% and 2.0 e$^-$/Å^3, respectively. Refined occupancies of 0.99(2), 1.00(2), and 0.98(2) for Ca1, Ca2, and Fe, respectively, correspond to a composition of $Ca_{4.98(4)}Pb_3Fe_{0.98(2)}$, and these were again set equal to unity in the final refinements.

The structural study of Ca_5Pb_3Cu showed it had only trigonal symmetry, in contrast to that of hexagonal Ca_5Pb_3Mn. This was not immediately clear from the powder data, but long-exposure precession photographs and data averaging revealed that the symmetry was indeed trigonal, with possible space groups $P\bar{3}c1$ and $P3c1$. Subsequent refinements indicated the correct space group was $P\bar{3}c1$. The initial refinement of the crystal structure presented many problems because of severe absorption effects poorly treated with only psi-scan data. This was manifested by elongated thermal parameters of all atoms. However, subsequent DIFABS corrections and anisotropic refinements led to a well-behaved solution, with $R/R_w = 3.0/4.3\%$, a ΔF map residual of 3.32 e$^-$/Å^3, less than 1 Å from Pb, and a refined composition of $Ca_5Pb_{3.05(4)}Cu_{1.01(2)}$. The principal geometric differences from the hexagonal structure are 0.15 Å displacements of the Ca1 atoms (in the linear chain) along $\vec{c}$ and out of the (002) planes that otherwise also contain the interstitial atoms at $z = 0, {}^1/_2$. The possibility of Cu/Pb mixed occupancies was considered, but these resulted in unsatisfactory R values.

A summary of some crystal and refinement data and the atomic parameters for all three structures are given in Tables 3 and 4, respectively. More data beyond those in Table 3 and the anisotropic displacement parameters for all three structures are contained in the Supporting Information (SI). These and the F_o/F_c tabulations are also available from J.D.C.

Table 3. Some Data Collection and Refinement Parametersa

	Ca_5Pb_3Mn	Ca_5Pb_3Fe	Ca_5Pb_3Cu
fw	876.93	877.84	885.54
space group	$P6_3/mcm$ (No. 193)	$P6_3/mcm$ (No. 193)	$P\bar{3}c1$ (No. 165)
Z	2	2	2
D, g cm^{-3}	5.46	5.49	5.44
μ (Mo Kα, cm^{-1})	757	787	550
R,b %	3.7	3.2	3.0
R_w,b %	3.9	3.5	4.3

a Cell parameters are in Table 1. b $R = \Sigma||F_o| - |F_c||/\Sigma|F_o|$; $R_w = [\Sigma w(|F_o| - |F_c|)^2/\Sigma w(F_o)^2]^{1/2}$; $w = F_o^{-2}$.

Results and Discussion

Syntheses. The high-yield syntheses, chemical analyses (Table 2), and the X-ray results (Tables 1 and 3) make clear that the series of stoichiometric compounds Ca_5Pb_3Z exist for interstitial Z = V, Cr, Mn, Fe, Co, Ni, Zn, Ru, or Cd.

(26) Blöchl, P. E.; Jepsen, O.; Andersen, O, K. *Phys. Rev. B* **1994**, *49*, 16223.
(27) Dronskowski, R.; Blöchl, P. *J. Phys. Chem.* **1993**, *97*, 8617.
(28) Hughbanks, T.; Hoffmann, R. *J. Am. Chem. Soc.* **1983**, *105*, 3528.
(29) TEXSAN, version 6.0; Molecular Structure Corp.: The Woodlands, Texas, 1990.
(30) Walker, N.; Stuart, D. *Acta Crystallogr.* **1983**, *A39*, 158.

Table 4. Positional Parameters and Isotropic-Equivalent Ellipsoidal Data

atom	x	y	z	B_{eq}[a]
		Ca_5Pb_3Mn		
Pb	0.6117(1)	0	3	2.98(6)
Ca1	1/3	2/3	0	1.4(2)
Ca2	0.2649(4)	0	1/4	2.4(3)
Mn	0	0	0	3.5(3)
		Ca_5Pb_3Fe		
Pb	0.6108(1)	0	1/4	2.58(5)
Ca1	1/3	2/3	0	1.6(1)
Ca2	0.2640(4)	0	1/4	2.6(2)
Fe	0	0	0	3.7(2)
		Ca_5Pb_3Cu		
Pb	0.6108(2)	0	1/4	2.9(1)
Ca1	1/3	2/3	0.021(1)	1.62(1)
Ca2	0.2643(6)	0	1/4	3.3(2)
Cu	0	0	0	4.2(1)

[a] $B_{eq} = (8\pi^2/3)\Sigma_i\Sigma_j U_{ij} a_i a_j a_i a_j$.

These are isostructural with the large variety of stuffed Mn_5Si_3Z-type compounds, the essential chain structure of which is shown in Figure 1. At first glance, the mere existence of these compositions in a structure with nominally isolated lead anions (d(Pb−Pb) ∼ 4.08 Å) seemed to require that these interstitials formally donate two electrons to the bonding (valence) manifold in order to achieve closed configurations for Pb. However, this view turns out to be too extreme in light of the strong Ca−Pb bonding and the absence of a closed lead p band for either Z = Mn or Cu that is described later. It seems noteworthy that this series of compounds occurs only with lead and the smallest high-lying countercation (Ca) of any of the hosts broadly examined to date, particularly, that no analogue could be found in any of the related ternary $(Sr,Ba)_5(Sn,Pb)_3Z$ or Ca_5Sn_3Z systems.[31] All of these absences seem subject to explanation as well (below). Also, attempts to incorporate Li, K, Mg, or many conventional main-group element interstitials (Ge, Si, P, Sb, S) as potential Z atoms did not yield any corresponding Ca_5Pb_3Z phases. In particular, attempts to make the analogous Ca_5Pb_3Mg with an ion comparable in size to divalent Co, Ni, Cu, and Zn led instead to substitution of Mg on Ca sites in a ternary mixed cation variant of the orthorhombic Co_2Si-type structure, $(Ca_5Mg)Pb_3$. The same structure type exists as Ca_5SrPb_3 as well as for a larger family of $Ca_{2-x}Mg_xSn$ phases for $x \leq 1.0$.[32]

The Normal Structure. Figure 1 shows the unit cell in a [001] projection of Ca_5Pb_3Fe, and a [110] section in Figure 2 details the arrangement of lead between the two cation chains. The confacial chains of trigonal antiprismatic Ca2 (blue), centered by Fe (black) and edge-bridged by Pb (red), run along (0,0,z) with Ca1 (light blue) lying within twisted Pb antiprisms (not marked) in linear strings along $^1/_3$, $^2/_3$, z, etc. In comparison with the electron-richer La_5Ge_3Cr, the distances between M atoms in adjoining triangular faces of M_6Z (the side edges of the trigonal antiprisms) are larger by 0.13 Å, 4.287 Å (Ca, Table 5) vs 4.160 Å (La).[8] On the other hand, the edges of the shared faces in the two are

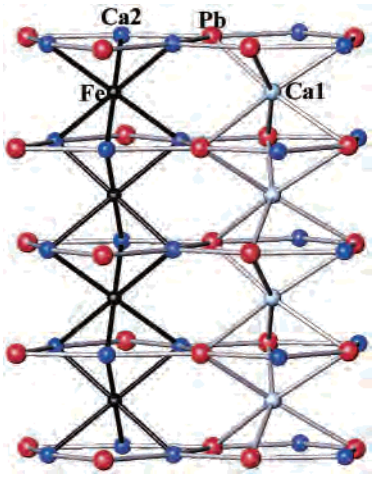

Figure 2. ∼[110] section of the structure of Ca_5Pb_3Fe showing the interlinked parallel antiprismatic $(Ca2)_6Fe$ (left) and $Ca(1)Pb_{6/2}$ (right) chains. Atom scheme is the same as in Figure 1.

Table 5. Nearest Neighbor Distances in Ca_5Pb_3Z, Z = Mn, Fe, Cu

		Ca_5Pb_3Mn	Ca_5Pb_3Fe		Ca_5Pb_3Cu
Pb−Ca1	6×	3.3854(3)	3.382(1)	3×	3.329(7)
				3×	3.482(8)
Pb−Ca2		3.246(2)	3.244(2)		3.26(1)
Pb−Ca2	2×[a]	3.216(1)	3.219(1)		3.240(3)
Pb−Ca2	2×[b]	3.690(2)	3.695(2)		3.715(4)
Pb−Pb	2×	4.0809(1)	4.072(1)		4.096(2)
Ca1−Ca1	2×	3.5045(5)	3.5045(5)		3.526(1)
Ca1−Ca2	6×	3.900(2)	3.903(2)	3×	3.861(9)
				3×	3.99(1)
Ca2−Ca2	4×	4.292(1)	4.287(1)		4.316(7)
Ca2−Ca2	2×[a]	4.294(1)	4.277(2)		4.31(2)
Ca2−Z	2×	3.036(3)	3.028(3)		3.05(1)
Z−Z	2×	3.5045(5)	3.5045(5)		3.526(1)
Ca1−Z	2×		5.401(2)		5.437
Pb−Z	2×	4.034(1)	4.041(1)		4.065(2)

[a] Normal to $\vec{c}$. [b] Intrachain.

markedly disparate, 4.277 Å for Ca vs only 3.751 Å for La, a 0.53 Å difference. Thus, substantially greater repulsions or weaker bonding or both seem evident in the Ca cages in Ca_5Pb_3Fe, and the Mn compound is even more extreme in the second difference.. Somewhat more electropositive interstitials might seem indicated, but it is also noteworthy that these phases are nominally also the poorest in excess electrons that we have been able to study in this structure type. The Ca−Z distances are relatively large as well; the La−Cr distance in La_5Ge_3Cr[8] is 0.075 Å less than the sum of single bond metallic radii, whereas d(Ca−Mn) here is 0.12 Å *greater*. (In comparison, the crystal[33] and metallic[34] diameters of Ca vs La differ by only 0.04 and 0.08 Å, respectively, La and Ca being the larger in the respective measures.)

Copper and Silver Interstitials. Exploratory studies with copper and, especially, silver were test cases since +2 oxidation states would scarcely be expected, these essentially requiring an unlikely oxidation of Cu^I and Ag^I by holes in the valence band of lead. Both compounds occur in a topologically identical structure in the maximal subgroup

(31) Harp, J. G., M. S. Thesis, Iowa State University, 1994.
(32) Ganguli, A. K.; Guloy, A. M.; Corbett, J. D. *J. Solid State Chem.* **2000,** *152*, 474.
(33) Shannon, R. D. *Acta Crystallogr.* **1976**, *A32*, 751.
(34) Pauling, L. *Nature of the Chemical Bond*, 3rd ed.; Cornell Press: New York, 1960; p 400.

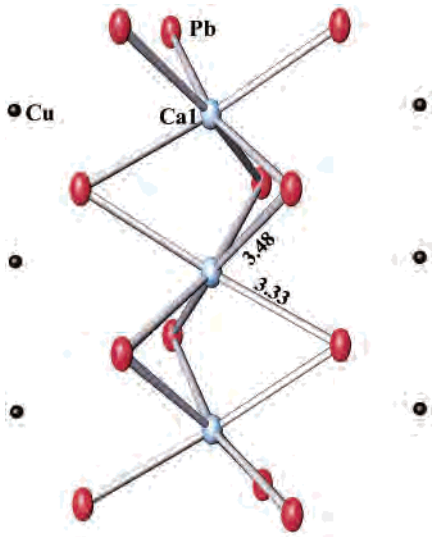

Figure 3. The slightly asymmetric chain of $Pb_{6/2}Ca(1)$ that lies along $^1/_3$, $^2/_3$, z, etc. in Ca_5Pb_3Cu ($P\bar{3}m1$). The lead atoms shown also bridge edges normal to the confacial chains of $Ca(2)_{6/2}Cu$ (Figure 2) (50% probability ellipsoids). The atom color scheme is the same as in Figure 1.

$P\bar{3}c1$. The only significant change occurs for the Ca1 atoms in the isolated chains at $^1/_3$, $^2/_3$, 0 and $^2/_3$, $^1/_3$, 0, etc. along $\vec{c}$, which have alternately moved along c by ± 0.15 Å (for Cu) so that they are no longer coplanar with close packed layers containing interstitial Cu (Figure 2). This vertical displacement of the Ca1 atoms within the twisted Pb_6 trigonal antiprisms is barely discernible in the section of both chains in Figure 3. The proportions of the Ca2 antiprisms around Cu are now slightly more extreme than those with Fe and Mn, such that the axial and equatorial Ca2−Ca2 distances are both 0.03 Å greater than those in Ca_5Pb_3Fe. We presume this is associated with the larger Cu interstitial as the d bands are filled and lower in energy. Once one knows where to look, the Guinier powder pattern of Ca_5Pb_3Cu, etc. may be distinguished from those of the Mn_5Si_3Z type by very weak extra lines, principally those with (122), (321), and (141) indices, all of which have $I/I_{max} < 0.02$.

Physical Properties. The magnetic and transport properties of some Ca_5Pb_3Z compounds, as well as core binding energies of Fe in a series of related compounds, offer significant support that these phases are very different from those studied before in which more screened or more anion-like states of Z seem evident. Magnetic susceptibility data of Ca_5Pb_3Mn (single phase in the powder pattern) are substantially temperature-independent, with a mean of 1.3×10^{-2} emu/mol, decreasing slightly over 50−295 K. This is larger by a factor of ∼3−4 than for typical Pauli-like behavior, and we do not understand it. The resistivity of Ca_5Pb_3Mn, $\rho_{295} \sim 130$ $\mu\Omega$ cm with a temperature dependence of $+0.42\%$ K^{-1}, is reasonable for a poor metal. These characteristics of Ca_5Pb_3Z would seemingly contradict a simple Zintl model in which a cationic nature of Z was necessary to complete the 6p valence shell of Pb. Although a metallic characteristic alone is not immediately a strong contradiction of the Zintl picture, particularly among salts of more complex trielide clusters,[35,36] it is more telling in the presence of a supposedly simple Pb^{-4} anion. The calculations that follow make it clear that the lack of a stable closed-shell configuration for lead is prime reason for the metal-like properties.

The compound Ca_5Pb_3Fe is strongly attracted to a permanent magnet at room temperature and remains ferromagnetic to above 200 °C. The observed moment of 6.3(1) μ_B mol^{-1} is strikingly near that for $Fe^{II}(^5T_2)$, 6.7 μ_B (for j−j coupling),[37] rather than the high-spin-only value of 4.9 μ_B. The compound is a very soft ferromagnet (as is La_5Ge_3Fe[20]), with no hysteresis and zero values of coercivity and remanence within experimental error (±2 Oe). Electron coupling within the chains might be expected just via the bonding Fe 4s states (d(Fe−Fe) = 3.50 Å), and at least good coupling between the antiprismatic chains could be achieved via conduction electrons in Pb states, atoms that are common neighbors, bridging edges on one chain and exo-bonding to another (Figure 1). A less screened character for Fe seems indicated when the 6.3 μ_B moment is compared with those of the electron-richer metallic $La_{15}Ge_9Fe$ (a $\sqrt{3} \times \sqrt{3}$ superstructure of La_5Ge_3Fe); 1.83, La_5Ge_3Fe, 1.93;[20] and Fe, 2.0 μ_B.[37]

Along the same lines, the core binding energy of iron $2p_{3/2}$ in Ca_5Pb_3Fe, 707.2 eV, is equally suggestive of relative valence electron loss or oxidation from related intermetallics if 705.8 and 705.3 eV binding energies in the electron-richer La_5Ge_3Fe, and $La_{15}Ge_9Fe$,[20] respectively, are compared with 706.4−709.2 eV for $Fe(CN)_6^{4-}$, FeS_2, and FeO as a group and 707.0 eV for Fe.[38]

Regarding the distorted copper and silver derivatives, the latter is the largest Z incorporated, and it expands the structure primarily along the a direction. The copper phase is weakly diamagnetic, around -6×10^{-6} emu mol^{-1}, which is zero within expected core correction errors. On the other hand, Ca_5Pb_3Ag does appear to be Pauli paramagnetic, $\chi_M = 3.66 \times 10^{-4}$ emu mol, decreasing only 0.5% over 50−295 K (SI).

Bonding. The electronic structure of Ca_5Pb_3Mn is characterized by energetically low-lying, well-localized Pb s states, as seen in the band and DOS data in Figure 4. At higher energies, a broad region of Pb p bands results that extends beyond the Fermi level. These bands show significant contributions from Ca d states (along with some s and p character), as outlined with the dashed projection in the DOS summary. The strongest Mn contribution to the overall DOS around E_F comes from a narrow band of d states (dotted projection). Mn s states occur in the lower part of the Pb p conduction band, and their contributions around the Fermi level are almost negligible. The COHP analyses in Figure 5

(35) Corbett, J. D. In *Chemistry, Structure and Bonding of Zintl Phases and Ions*; Kauzlarich, S., Ed.; VCH Publishers: New York, 1996; Chapter 3.
(36) Nesper, R. *Prog. Solid State Chem.* **1990**, *20*, 1.
(37) Carlin, R. L. *Magnetochemistry*; Springer-Verlag: Berlin, Germany, 1986.
(38) Moulder, J. F.; Stickle, W. F.; Sobel, P. E.; Bomben, K. D. *Handbook of X-ray Photoelectron Spectroscopy*; Perkin-Elmer Corp.: Eden Prairie, MN, 1992.

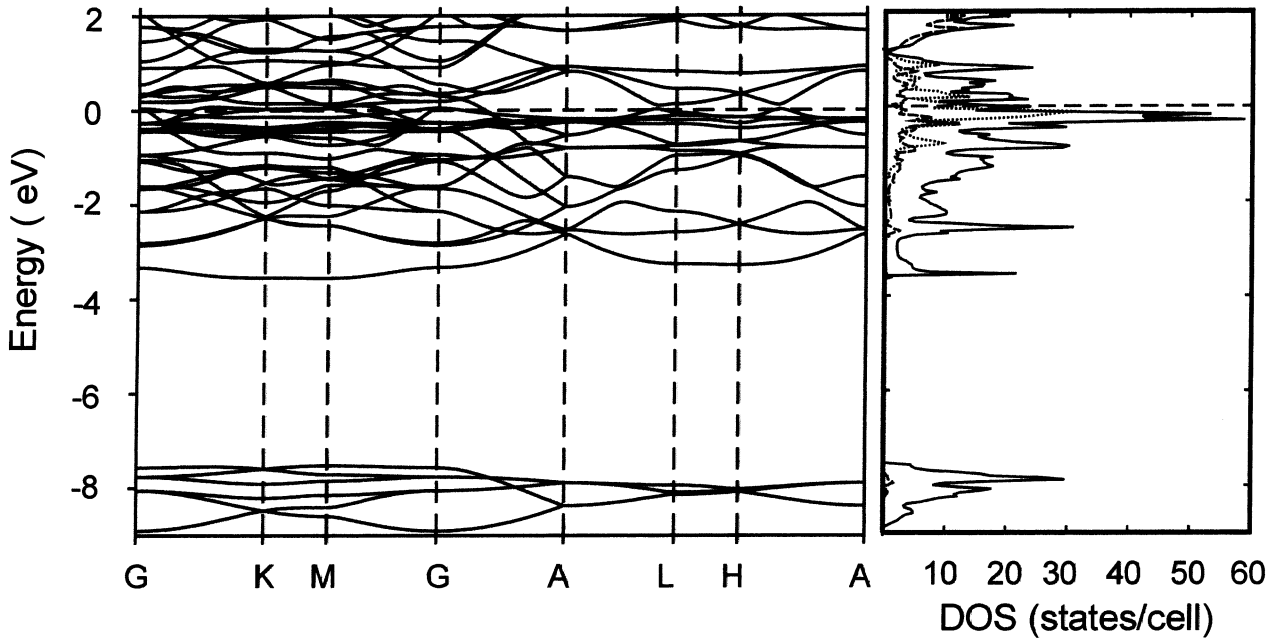

Figure 4. Band structure (left) and DOS (right) for hexagonal Ca_5Pb_3Mn. The inserts on the right side are Mn d (dotted) and Ca d (dashed).

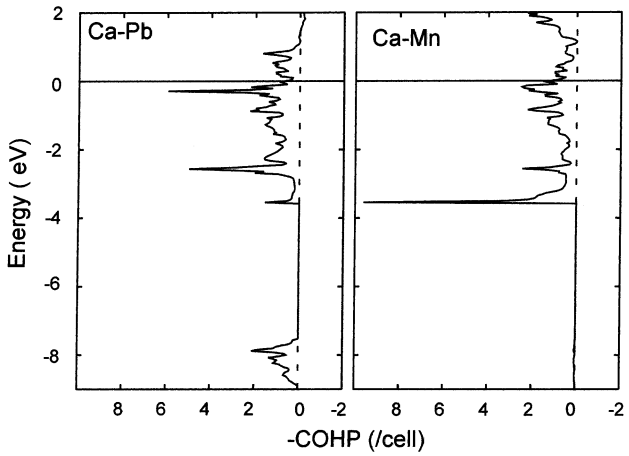

Figure 5. COHP ($cell^{-1}$) vs energy (eV) in Ca_5Pb_3Mn for Ca−Pb (left) and Ca−Mn (right).

for all Ca−Pb (left) and Ca−Mn (right) interactions show strongly bonding Ca−Pb interactions around and, especially, just below the Fermi level. More localization and strong bonding throughout this band, particularly below E_F, is provided by Ca−Mn interactions. Neither is optimized, the bonding states above E_F reflect the electron-poor nature of the system. There is no significant Ca−Ca or Pb−Pb bonding.

The eminent role of the interstitial in these structures becomes obvious on comparison of the band structure calculational results for Ca_5Pb_3Mn with those for a hypothetical empty Ca_5Pb_3 in the same structure type. Aside from the obvious fact that the d states of the added Mn atoms give rise to a higher DOS around the Fermi level, the band dispersions are generally larger in the filled Mn_5Si_3X structures because of additional strong interatomic interactions. A noteworthy circumstance in the case of the Mn-stuffed Ca_5Pb_3 is that the Fermi level falls at a local minimum for both the Pb and Ca states, suggesting optimized bonding. In strong contrast, an absolute maximum in DOS is reached at E_F in the empty structure, just below a deep minimum. COHP analyses show stronger Ca−Pb interactions in the stuffed compound plus additional bonding contributions from Pb−Mn interactions (especially between the Mn s and Pb p states). Thus, stuffing Ca_5Pb_3 with manganese leads to a substantial enhancement of the overall bonding, an effect that is evidenced in a very general sense by the considerable number of stuffed Mn_5Si_3-type examples that are known.[2]

The band structures of Ca_5Pb_3Mn and Ca_5Pb_3Cu are very much alike; at first sight, the host atom contributions remain unaffected when the interstitial is exchanged. The big difference lies in the higher electron count and electronegativity of copper. Copper strongly favors a closed d^{10} shell and, in contrast to the situation with Ca_5Pb_3Mn, those levels form a narrow, well-localized band in the lower regions of the Pb−Ca conduction band about 2.5 eV below E_F (Figure 6). The Cu s states occur mainly at even lower energies, but they show a higher dispersion that reaches across the Fermi level. The small distortion observed in the Cu and Ag salts, lowering the symmetry to $P\bar{3}ml$, consists mainly of a 0.15-Å displacement of Ca1 along $\vec{c}$ in the Cu structure. Changes in bands and DOS curves are quite small, as seen in Figure 6 (Cu) vs Figure 4 (Mn), but an energy gain for the former is found on inspection of the before-and-after COHP curves for Ca−Pb (top) and Ca−Cu (bottom) rows in Figure 7 as a function of the real (right pair) and the ideal undistorted (left) Ca_5Pb_3Cu structures.

The Ca−Pb interactions are comparable in both, but with the electron-richer Cu, the Ca−Cu interactions (bottom pair) change across the energy scale from bonding to antibonding at the top of the Cu d band and back to slightly bonding at E_F. Distortion of the structure by moving Ca1 off the symmetry center and increasing the Ca1−Cu distance by only 0.02 Å leads to an improvement in the bonding by reducing the Ca−Cu antibonding interactions around −2.5

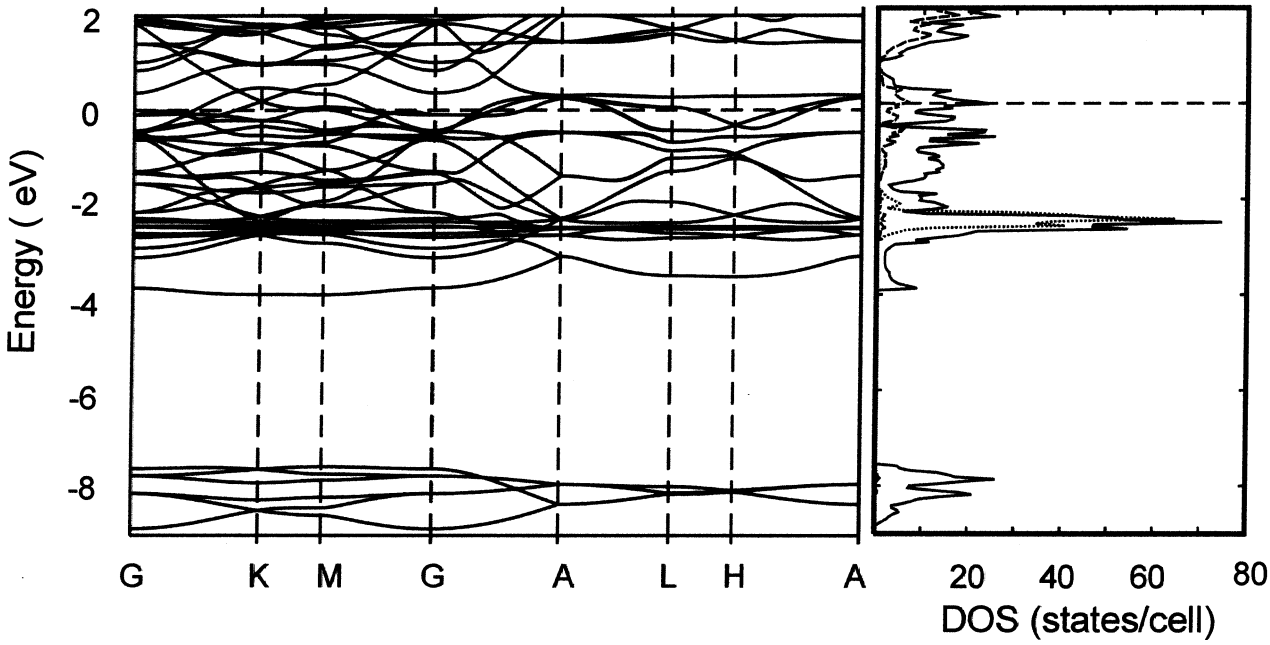

Figure 6. Band structure (left) and DOS (right) for the distorted Ca_5Pb_3Cu. Projections on the right side are Cu d (dotted) and Ca d (dashed).

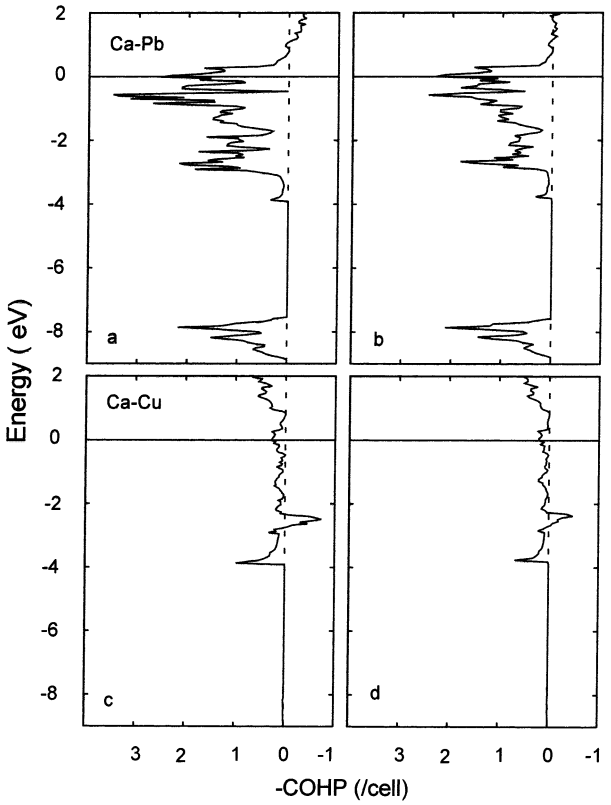

Figure 7. COHP as a function energy for Ca−Pb and Ca−Cu in Ca_5Pb_3CU: Left column (a, c), bonding in ideal ($P6_3/mcm$) structure; right column (b, d), bonding in observed ($P\bar{3}m1$) structure; Top row (a, b), bonding for Ca−Pb in ideal and observed structures; bottom row (c, d), bonding for Ca−Cu in ideal and observed structures, respectively.

eV, which gives an increase in net (integrated) Ca−Cu bonding interactions by a factor of over 2.8 (0.13 eV/cell). At the same time, the total Ca1−Pb bonding is strengthened, Figure 7, top pair. Thus the distortion of the basic stuffed Mn_5Si_3 structure has electronic origins for this electron-rich 3d interstitial and presumably also for Ag. Madelung calculations (Ewald method) show that the observed distortion from the ideal Mn_5Si_3 type host is also slightly favored by reduced repulsions between Cu and Ca1.

It has already been shown that the simple concept of closed shell Zintl monoanions for the heavier elements does not hold true in the presence of countercations that have low lying d orbitals, alkaline-earth and rare-earth elements, particularly. Thus, an interstitial in the Ca_5Pb_3Z series does not act as an electron donor and fill the valence shell of the anion but instead just enhances both the bonding interactions within the respective compound, especially Ca−Z and, presumably, the Madelung energy. Like compounds with more electronegativity and electron-demanding Z atoms (Ge, Si, Sb, S) logically do not form.

Comparison of the foregoing with results of EHTB calculations on La_5Ge_3Fe[8] emphasizes the differences. The apparent bond strengths (overlap populations) clearly show that La−Fe > La−Ge, whereas the opposite is true here for overlap populations, Ca−Pb > Ca−Mn, again consonant with the greater polarizability of Pb and the weaker bonding of Mn. In the La_5Ge_3Fe compound, E_F again cuts across a high DOS. As far as related systems, a change from Ca to Sr or Ba causes phase instability, presumably from decreases in the same contributions. Although d levels on the cations come down in energy and give better mixing with Pb states, their polarization of the anion and Madelung contributions also decrease.[16] The nonexistence of the corresponding Sn compounds presumably results from a clear tendency for that element to form the relatively more stable closed-shell Sn^{-4} state as a monoanion. An opposite effect for the same reasons has been observed for Sb vs Bi in the Ae_4Pn_3 systems with inverse-Th_3P_4 structures; the Sb analogues and all Ca examples are unknown with respect to other phases, whereas

(39) Li, B.; Mudring, A.-V.; Corbett, J. D. *Inorg. Chem*., in press.

stable open shell (Ba, Sr)$_4$Bi$_3$ phases are known[39] for many of the same reasons.

Good conductivity tests for other compounds containing nominally anionic lead are difficult to find. There are numerous examples of rare-earth metal−lead compounds with discrete mono- or di-lead anions in Mn_5Si_3, Sm_5Ge_4, or Zr_5Si_4 structure types, but most of these are electron rich and naturally metallic. A rather unusual case is the seemingly valence precise compound La_5Pb_3N that features only Pb monomers.[40] Its conductivity is unknown, but from what we have found before, a metallic behavior seems probable with this particular combination of metals. It would not be surprising if the long known $(A^+)_4Pb_4^{-4}$ Zintl phases were to be metallic (as is Na_4Sn_4[41]), while Ae_2Pb[42] and Li_2MgPb[43] are metallic by experiment and theory, respectively. We measured the resistivity of what would seem to be a prime lead(−IV) prospect for semiconduction, Ca_3PbO with its inverse perovskitic structure, and found it to be metallic ($\rho_{298} = -57\ \mu\Omega$ cm, 0.08% K^{-1}).[44] Theory is also in accord.[43]

Summary. The family of transition-metal-interstitial compounds Ca_5Pb_3Z (Z = V, Cr, Mn, Fe, Co, Ni, Zn, Ru, Cd, Cu, or Ag) represents a new type of filled-Mn_5Si_3 structures, the Z atoms at first glance seeming to behave more as nominal, formal electron donors. However, the fallacy lies in the assumption of a closed shell Pb^{-4} state, which does not happen. LMTO band structure calculations indicate that strong Ca−Pb and lesser Ca−Mn bonds, both with significant Ca d mixing, dominate the chemical bonding in the isostructural Ca_5Pb_3Z phases. The formation of this series of ternary compounds and the absence of the binary Ca_5Pb_3 example must result from the gains in both specific Ca−Z bonds with the small cation and a gain in Madelung energy. With filled 3d shells, the Cu and Ag analogues are both distorted in a direction that appears to strengthen the Ca−Pb bonding in the host and to reduce Z−Ca1 repulsions. The successful incorporation of a variety of transition metals provides a useful handle in modulating the structural and physical properties of the binary Ca_5Pb_3 "host".

Acknowledgment. A.V.M. thanks the A. v. Humboldt Foundation for a Feodor Lynen Fellowship. We gratefully acknowledge R. A. Jacobson for use of X-ray facilities, J. Shinar for the Q measurements, J. Anderegg for his valuable help on the XPS measurements, A. F. Guloy for the microprobe/XPS analyses, and J. Ostenson for the magnetic susceptibility measurements.

Supporting Information Available: Tables of additional diffraction and refinement data, anisotropic displacement parameters for the three structures, and magnetic data for Ca_5Pb_3Cu and Ca_5Pb_3Ag. The material is available free of charge via the Internet at http://pubs.acs.org.

IC0301728

(40) Guloy, A. M.; Corbett, J. D. *Z. Anorg. Allg. Chem.* **1992**, *616*, 61.
(41) Nesper, R. Private communication.
(42) van Attekum, P. M.; Wertheim, G. K.; Grecelius, G.; Wernick, J. H. *Phys. Rev. B* **1980**, *22*, 3998.
(43) Mudring, A.-V.; Corbett, J. D. Unpublished research.
(44) Klem, M. T.; Corbett, J. D. unpublished research, 2001.